Functional parameterization for hydraulic conductivity inversion with uncertainty quantification

Jianying Jiao & Ye Zhang

🐎 Springer

Springer

Functional parameterization for hydraulic conductivity inversion with uncertainty quantification

Jianying Jiao · Ye Zhang

Abstract Functional inversion based on local approximate solutions (LAS) is developed for steady-state flow in heterogeneous aquifers. The method employs a set of LAS of flow to impose spatial continuity of hydraulic head and Darcy fluxes in the solution domain, which are conditioned to limited measurements. Hydraulic conductivity is first parameterized as piecewise continuous, which requires the addition of a smoothness constraint to reduce inversion artifacts. Alternatively, it is formulated as piecewise constant, for which the smoothness constraint is not required, but the data requirement is much higher. Success of the inversion with both parameterizations is demonstrated for both one-dimensional synthetic examples and an oil-field permeability profile. When measurement errors are increased, estimation becomes less accurate but the solution is stable, i.e., estimation errors remain bounded. Compared to piecewise constant parameterization, piecewise continuous parameterization leads to more stable and accurate inversion. Moreover, conductivity variation can also be captured at two spatial scales reflecting sub-facies smooth-varying heterogeneity as well as abrupt changes at facies boundaries. By combining inversion with geostatistical simulation, uncertainty in the estimated conductivity and the hydraulic head field can be quantified. For a given measurement dataset, inversion accuracy and estimation uncertainty with the piecewise continuous parameterization is not sensitive to increasing conductivity contrast.

Keywords Groundwater flow · Inverse modeling · Direct method · Hydraulic conductivity · Uncertainty

Introduction

Hydraulic conductivity (K) is a key parameter influencing fluid flow and solute transport in aquifers. Accurate

J. Jiao · Y. Zhang (✉)
Department of Geology and Geophysics,
University of Wyoming, Laramie, WY 82071, USA
e-mail: yzhang9@uwyo.edu

estimation of aquifer conductivity is a challenging task, however, due to issues related to aquifer heterogeneity, parameter and measurement scale effect, uncertainty in aquifer boundary conditions (BC), and the lack of efficient estimation techniques. In modeling groundwater flow, besides conductivity, aquifer BC also need to be ascertained which are typically poorly known (in transient analysis, initial condition is also required). In hydrogeology, the estimation of aquifer conductivity and the assignment of appropriate initial and boundary conditions are commonly addressed with the inverse method, which according to Sagar et al. (1975), can be categorized into five types based on the types of unknowns: (1) model parameters, (2) initial conditions, (3) boundary conditions, (4) sources and sinks, and (5) a mixture of the preceding. This article addresses type 5 inversion by estimating aquifer conductivity and BC simultaneously, for which K is parameterized as a set of functions in the inversion grid. Such functions can be piecewise continuous or piecewise constant, the latter parameterization is similar to those adopted in inverting highly parameterized problems (Zhou et al. 2014). Moreover, by combining type 5 inversion with geostatistical simulation, uncertainty in the estimated conductivities and the flow will be quantified. Sources/sinks, such as pumping and recharge, are not addressed, thus problems investigated here pertain to the aquifer monitoring condition where ambient flow dominates.

The majority of the existing inverse methods fall into those of type 1 or parameter estimation techniques (Yeh 1986; Ginn and Cushman 1990; McLaughlin and Townley 1996; Carrera et al. 2005; Hill and Tiedeman 2007; Vrugt et al. 2008). Typically, type 1 inversion adopts the indirect techniques which minimize a (regularized) measurement-to-model misfit, or an objective function. Such techniques may be classified into three kinds: classic, highly parameterized, and hybrid. In the classic approach, a model can be divided into a number of pre-defined zones, with each zone characterized with homogeneous parameters. A limited number of parameters are sought during calibration, sometimes with the goal of identifying the most parsimonious model. The classic approach has been implemented in a number of model-independent computer programs (e.g., UCODE and PEST) that are widely used in practice (Poeter et al. 2005; Hill 1992; Doherty 2005). Highly parameterized methods typically have many more parameters to estimate

598

than there are observations and can be divided into deterministic and stochastic approaches. A representative of the former is the Pilot Point estimation method (Doherty 2005); that of the latter is based on geostatistical inverse theory, where stochastic simulation, in addition to estimation, can be used to describe parameter variations and their probabilistic uncertainty (Carrera and Neuman 1986a,b,c; Kitanidis 1995; Yeh et al. 1996; Zimmerman et al.; 1998; Capilla et al. 1999; Medina and Carrera 2003; Janssen et al. 2006; Zanini and Kitanidis 2009). Hybrid or evolutionary approaches have also been developed. For example, PEST can incorporate Pilot Points within a zonation scheme, with zone-by-zone calibration of many parameters. Pilot Point locations can be iteratively selected (LaVenue and Pickens 1992), while zonation patterns can be derived from calibration (Eppstein and Dougherty 1996; Roggero and Hu 1998; Gallo and Ravalec-Dupin 2000). Based on Kalman Filter, a variety of data fusion techniques have been developed, whereas parameters are updated recursively using recent or near-real-time measurements (Ferraresi et al. 1996; Porter et al. 2000; Zhu and Yeh 2006). Related developments in petroleum engineering have incorporated production data into reservoir history-matching, within either a geostatistical (Deutsch and Journel 1994; Wen et al. 2000) or optimization framework (Romero et al. 2000; Schulze-Riegert et al. 2002; Kromah et al. 2005; Eide et al. 1994; Amudo et al. 2008).

The aforementioned estimation techniques differ in their implementation, although a common theme is the building and calibration of a forward model with which model fit against field observations is iteratively improved until model parameters are determined. Because a forward model is needed to evaluate the objective functions, aquifer BC need to be ascertained prior to parameter estimation. However, due to data limitation, BC are often poorly known and, as demonstrated in Irsa and Zhang (2012), BC calibration can lead to non-unique estimation of aquifer parameters and flow field. To address this issue, a direct method was recently developed for inverting steady-state flows, where analytical solutions of the groundwater flow equation (i.e., fundamental solutions of inversion) were used to enforce fluid flow continuity in space (Irsa and Zhang 2012; Zhang 2014; Jiao and Zhang 2014a; Jiao and Zhang 2014b; Zhang et al. 2014). The direct method does not require forward simulations to assess measurement-to-model misfits; thus the knowledge of aquifer BC is not required. Measurements used in the inverse model include hydraulic heads, Darcy fluxes, and pumping rates. Given sufficient (although limited) measurements, the direct method yields a set of well-posed systems of linear or nonlinear equations that can be solved efficiently with optimization. The method is thus computationally efficient and the solution includes the simultaneous estimation of conductivities and flow field (i.e., hydraulic head and Darcy flux) including the unknown BC. For transient flows, Jiao and Zhang (2014c) extended the earlier techniques by adopting a set of local approximate solutions (LAS) of flow as the fundamental solutions of inversion. Hydraulic conductivities, storage coefficients, BC, as well as the unknown aquifer initial conditions can be estimated. Finally, because the direct method does not simulate the forward model, a separate grid is developed for the inverse analysis and is referred to herein as the "inversion grid".

This grid can employ flexible discretization, which directly influences inversion parameterization.

In previous works by the authors, under-determined inversion can lead to unstable or non-converging solutions (Zhang 2014), thus *K* was parameterized using zonation, i.e., piecewise constant over groups of inversion cells. This approach ensures that the inverse systems of equations are exact or over-determined when measurements are limited. However, *K* of natural aquifers varies in a complex and irregular manner with local trends reflecting sediment grain size variations (Gelhar 1992). Large aquifer systems can contain multiple facies where *K* varies relatively smoothly within facies, but exhibits abrupt changes at their boundaries (Fogg 1990; Scheibe and Freyberg 1995; Anderson 1997; Zhang et al. 2005; Ramanathan et al. 2010). In this study, by adopting piecewise functions to approximate *K* (one for each inversion grid cell), the LAS inverse method is extended to address more realistic aquifer heterogeneity that is not described well by zonation. With the new formulation, spatially variable *K* can be estimated along with the flow field based on limited measurements. Conductivity estimation is also successful for multi-facies systems, where *K* changes abruptly at facies boundaries. Moreover, by combining inversion with geostatistical simulation, uncertainty in the estimated conductivity and flow field can be quantified.

In this study, using synthetic aquifer problems with heterogeneous hydraulic conductivity distributions, accuracy and stability of the LAS inverse method employing functional parameterization is demonstrated. When *K* is piecewise continuous, to maintain a well-posed system of equations and to eliminate artifacts, a local smoothness constraint is added. Highly parameterized inversion (i.e., *K* is piecewise constant) is found to be a subset of the new inversion, although the local smoothness constraint is not needed. However, it requires a large number of measurements to make the problem well-posed, which is not practical unless additional regularizations are used. For the synthetic problems, inversion accuracy and stability of the two formulations are demonstrated and compared. Piecewise continuous formulation with the smoothness constraint is found to be more stable in addition to having a lower data requirement.

In the following, the inverse method is described, followed by results testing the method using synthetic problems. Different *K* parameterizations, data supports, and measurement errors are tested. The inverse solution is considered stable if increasing measurement errors do not lead to unbounded errors in the estimated parameters and the flow field. The approach combining inversion with geostatistical simulation to quantify estimation uncertainty is described. Insights gained are summarized in sections 'Discussion' and 'Conclusion', where future research direction is also suggested.

Theory

The forward model

The steady state flow equation for a 1-D confined aquifer without source/sink effects can be written as:

$$\frac{\partial}{\partial z}\left(K(z)\frac{\partial h(z)}{\partial z}\right) = 0 \qquad \text{in } \Omega \tag{1}$$

$$q(z) = -K(z)\frac{\partial h(z)}{\partial z} \qquad \text{in } \Omega \tag{2}$$

where $h(z)$ is hydraulic head [L], $K(z)$ is hydraulic conductivity [L/T], Ω denotes the model domain, z is vertical axis [L], and $q(z)$ is Darcy flux [L/T]. Equations (1) and (2) are written for the vertical axis to reflect problems in inverting borehole data.

For the forward model, boundary conditions are Dirichlet-type:

$$h = g(z) \quad \text{on } \partial\Omega \tag{3}$$

where $\partial\Omega$ is Dirichlet model boundary and $g(z)$ describes a set of prescribed heads on the boundaries.

The LAS inverse model

The inverse method of this study enforces 4 constraints: (1) global continuity of hydraulic head and Darcy fluxes throughout the solution domain; (2) conditioning of the LAS to observed hydraulic heads and Darcy fluxes; (3) a set of equation constraints, imposed at selected points in the inversion grid; (4) continuity of K at selected locations according to the characteristics of heterogeneity. The last constraint is implemented in the inverse formulation with a piecewise continuous parameterization, but is not needed for the piecewise constant inversion.

The first constraint can be written as a set of continuity equations of hydraulic head and Darcy's flux:

$$\int R_h(\Gamma_j)\delta\left(p_j-\varepsilon\right)d\Gamma_j = 0, \; j = 1,...,Y \tag{4}$$

$$\int R_q(\Gamma_j)\delta\left(p_j-\varepsilon\right)d\Gamma_j = 0, \; j = 1,...,Y \tag{5}$$

$$R_h(\Gamma_j) = h^i(\Gamma_j) - h^k(\Gamma_j) \tag{6}$$

$$R_q(\Gamma_j) = q^i(\Gamma_j) - q^k(\Gamma_j) \tag{7}$$

where h and q are a set of proposed fundamental solutions of inversion (i.e., LAS in this work, introduced later), i and k denote cells in the inversion grid adjacent to a cell interface Γ_j, $R_h(\Gamma_j)$ and $R_q(\Gamma_j)$ are residuals of h and q at Γ_j, respectively, Y is the total number of cell interfaces, and $\delta\left(p_j-\varepsilon\right)$ is the Dirac delta weighting

function which samples the residuals at a set of collocation points on Γ_j. In 1D inversion, only one collocation point exists per cell interface, thus the total number of collocation points is Y.

In the second constraint, the LAS are conditioned by local measurements of hydraulic head and flux:

$$\delta(p_a-\varepsilon)\left(h(p_a)-h_a^o\right) = 0 \qquad a = 1,...,A; \tag{8}$$

$$\delta(p_b-\varepsilon)\left(q_x(p_b)-q_b^o\right) = 0 \qquad b = 1,...,B; \tag{9}$$

where p_a and p_b are measurement points, h_a^o and q_b^o are observed hydraulic head and Darcy flux at p_a and p_b, respectively, A and B are the number of observed heads and fluxes, respectively, $\delta(p_a-\varepsilon)$ and $\delta(p_b-\varepsilon)$ are weighting functions assigned to reflect the magnitude of the measurement errors. In general, $\delta(p_a-\varepsilon)$ and $\delta(p_b-\varepsilon)$ are proportional to the inverse of error covariance. To evaluate the accuracy and stability of inversion, inverse solutions under both error-free and random measurement errors (with zero mean) are investigated.

To enforce the steady-state flow equation locally, a set of equation constraints is developed:

$$\delta(p_c-\varepsilon)R_c = 0; \qquad R_c = \left[\frac{\partial}{\partial z}\left(K(z)\frac{\partial h(z)}{\partial z}\right)\right]\Bigg|_c \tag{10}$$

$$c = 1,...,Y+A+B$$

where p_c include both the collocation points and the measurement locations and R_c is residual of the flow equation at p_c. The equation constraint is needed because, as shown as below, the fundamental solutions of inversion are local approximate solutions, which allow the evaluation of general heterogeneous problems with significant boundary effects. At the p_c locations, Eq. 10 enforces a physical flow constraint on the LAS.

When K is parameterized as piecewise continuous, a set of continuity equations can be written at selected locations according to the characteristics of heterogeneity:

$$\int R_K(\Gamma_j)\delta\left(p_j-\varepsilon\right)d\Gamma_j = 0, \; j = 1,...,X$$
$$R_K(\Gamma_j) = K^i(\Gamma_j) - K^k(\Gamma_j) \tag{11}$$

where K is a local conductivity function (one for each inversion cell), $R_K(\Gamma_j)$ is residual of K at Γ_j, X is the number of inversion grid cell interfaces where K continuity is imposed ($X \leq Y$), and i and k denote cells in the inversion grid adjacent to Γ_j. Again, $\delta\left(p_j-\varepsilon\right)$ is a Dirac delta weighting function.

600

Fundamental solutions

In this study, conductivity is parameterized as piecewise functions, one for each inversion cell. (Alternatively, a function can be parameterized for individual facies consisting of a group of cells, which is not tested). Conductivity is thus spatially variable within each inversion cell. If Ωi denotes such a cell, $i=1,…, M$ (M is the number of inversion cells), Eqs. (1) and (2) can be rewritten as a set of local flow equations:

$$\frac{\partial}{\partial z}\left(K(z)\frac{\partial h(z)}{\partial z}\right) = 0 \qquad \text{on } \Omega i \tag{12}$$

$$q(z) = -K(z)\frac{\partial h(z)}{\partial z} \qquad \text{on } \Omega i \tag{13}$$

where $K(z)$, $h(z)$ and $q(z)$ are local spatial functions on Ωi . Because source/sink effects are not considered, a set of hydraulic head, conductivity, and Darcy flux functions can be proposed as an approximate solution of Eqs. 12 and 13:

$$h(z) = a_1 + a_2 z + a_3 z^2 \qquad \text{on } \Omega i \tag{14}$$

$$K(z) = a_4 + a_5 z + a_6 z^2 \qquad \text{on } \Omega i \tag{15}$$

$$q(z) = -\left(a_4 + a_5 z + a_6 z^2\right)(a_2 + 2a_3 z) \qquad \text{on } \Omega i \tag{16}$$

where $a_l(l = 1, …, 6)$ are unknown coefficients on Ωi , to be determined by inversion. Given Eqs. (14)–(16), Eq. (10) can be rewritten as:

$$\delta(p_c - \varepsilon)\left[2a_3\left(a_4 + a_5 z + a_6 z^2\right) + (a_2 + 2a_3 z)(a_5 + 2a_6 z)\right] = 0 \tag{17}$$

Because highly parameterized inversion (i.e., piecewise constant K in each inversion cell), as implemented in many classic techniques, is a subset of the functional parameterization inversion, Eqs. (12), (13), (14), and (16) can be rewritten as:

$$K_i \frac{\partial}{\partial z}\left(\frac{\partial h(z)}{\partial z}\right) = 0 \qquad \text{on } \Omega i \tag{18}$$

$$q(z) = -K_i \frac{\partial h(z)}{\partial z} \qquad \text{on } \Omega i \tag{19}$$

$$h(z) = a_1 + a_2 z + a_3 z^2 \qquad \text{on } \Omega i \tag{20}$$

$$q(z) = -K_i(a_2 + 2a_3 z) \qquad \text{on } \Omega i \tag{21}$$

where in each Ωi , its local conductivity (K_i) is assumed homogeneous, and $a_l(l = 1, 2, 3)$ are the unknown coefficients on Ωi . Accordingly, Eq. (10) can be rewritten as:

$$\delta(p_c - \varepsilon)2a_3 K_i = 0 \tag{22}$$

In the highly parameterized inversion, Eq. (11) is not enforced when assembling the inverse formulations.

Solution techniques

Depending on parameterization, the inverse system of equation is assembled by Eqs. (4)–(11) (piecewise continuous), or Eqs. (4)–(10) (piecewise constant). The equation systems can be under-determined, exact, or over-determined, depending on both the inverse parameterization and the number of measurements used to condition the inversion. For the problems of this study, all equation systems are over-determined, because under-determined problems generally yield poor results. Due to the nonlinearity in the LAS, the inverse system of equations is nonlinear and is solved with two gradient-based optimization algorithms, i.e., Levenberg-Marquardt and Trust-Region-Reflective. Both algorithms are implemented in a MATLAB nonlinear solver, *lsqnonlin*, which solves a nonlinear least-squares problem of the form (The Mathworks, 2012):

$$\min_x \|f(x)\|_2^2 = \min_x \left(f_1(x)^2 + f_2(x)^2 + \cdots + f_w(x)^2\right) \tag{23}$$

where x is the inverse solution containing the unknown parameters and the coefficients, w is the number of equations, $f_1(x), f_2(x), …, f_w(x)$ are the equations assembled. For the piecewise continuous parameterization, a_l $(l = 1, …, 6)$ are the unknowns for each inversion cell; for the piecewise constant parameterization, $a_l(l = 1, …, 3)$ and K_i are the unknowns for each cell. The optimization algorithms require that an initial guess of x be provided, which is generated by assigning to x random values bounded by the range of the observed heads.

The LAS method, similar to all inversion methods, may suffer ill-posedness when insufficient and/or noisy data are used to condition the inversion. Thus, the inverse solution may not exist, it may not be unique, and it may be unstable. With sufficient and accurate data that lead to exact or over-determined equation systems, the inverse problems are generally well-posed, leading to fast, stable, and accurate solutions.

Uncertainty quantification

Most indirect inverse methods, particularly those based on geostatistical techniques, can estimate parameters and flow

field as well as quantify their estimation uncertainties (e.g., Kitanidis 1995; McKenna and Poeter 1995). Though a variety of uncertainty quantification approaches exist (Tartakovsky 2013), stochastic inversion based on the geostatistical technique offers considerable flexibility in its ability to integrate a variety of static and dynamic data that can also exhibit spatial (and temporal) correlations. The direct method, when combined with a geostatistical approach, can also lead to quantification of the estimation uncertainty. For selected problems, variogram-based conditional simulation is combined with inversion to quantify these uncertainties (Fig. 1). Both the piecewise continuous and piecewise constant parameterizations will be tested. The conditional simulation will honor the observed hydraulic heads, while providing a large number of simulated "measurements" for inversion. These simulated heads will be of varying qualities, as those closer to the observed heads generally exhibit smaller errors. The observed fluxes are not subject to such an analysis because, compared to hydraulic heads, flux sampling is relatively rare, which can lead to poor geostatistical simulation outcomes. Along with the observed heads and the observed fluxes, the simulated heads are used in the inverse model, leading to an over-determined equation system and stable inversion. For each conditionally simulated hydraulic head field, one inversion system will be solved. Given a large number of the conditionally simulated hydraulic heads realizations, an ensemble of inverted K and hydraulic head fields will be created, which leads to quantification of the estimation uncertainty. For example, a metric quantifying the calibration uncertainty in hydraulic head can be computed as (Sakaki et al. 2009):

$$\sigma_{nh} = \frac{1}{n_{\text{obs}}} \sum_{i=1}^{n_{\text{obs}}} \frac{\sigma_i^{\text{est}}}{h_i^{\text{est}}} \qquad (24)$$

where n_{obs} is the number of actual observed heads, h_i^{est} is the ensemble mean of the inverted hydraulic heads at the ith observed head location, and σ_i^{est} is the associated ensemble hydraulic head standard deviation, assuming that the inverted hydraulic head distribution at each observed head location follows a Gaussian distribution. Note that a tradeoff exists between the number of observed heads (n_{obs}) and estimation uncertainty: when n_{obs} is small, uncertainty in the conditionally simulated heads will be large, which will lead to larger estimation uncertainty, and vice versa.

Similar to Eq. (24), a metric for quantifying the calibration uncertainty in hydraulic conductivity can be computed:

$$\sigma_{nK} = \frac{1}{n_K} \sum_{i=1}^{n_K} \frac{\sigma_i^{\text{est}}}{K_i^{\text{est}}} \qquad (25)$$

where n_K is the number of selected conductivity locations used for comparison (in this work, these locations coincide with the observed head locations), K_i^{est} is the ensemble mean of the inverted conductivities at the ith conductivity location, and σ_i^{est} is the associated conductivity estimation standard deviation.

Results

Based on synthetic heterogeneous aquifer problems, accuracy and stability of the LAS inverse method with piecewise continuous or constant parameterization is first demonstrated (deterministic inversion). The inverse method, when combined with conditional simulation, then leads to the quantification of estimation uncertainties (stochastic inversion). For both deterministic and stochastic inversion, the solution is verified by comparing the estimated hydraulic conductivity and the inverted hydraulic head profiles to those of the forward (true) models. Each forward model, which is simulated with the finite-difference method (FDM), is used to generate observations for inversion under a set of true model boundary conditions (herein, FDM denotes a forward model). Three FDMs, labeled as cases (A), (B), and (C), have been created. Their K distributions, computational domain, and true forward model BC are listed in Table 1. Note that to ensure accurate forward solutions, dense grids are used.

For selected cases, analysis is conducted to evaluate the stability of inversion under increasing measurement errors. Hydraulic heads sampled from the FDM are considered error-free. To impose measurement errors, $h^{\text{m}} = h^{\text{FDM}} \pm \Delta h$, where h^{m} is measured head used in the inverse model, h^{FDM} is head sampled from the FDM, and Δh is a random measurement error. The highest error imposed is ± 1 % of the total head variation in the FDM. Thus, for problems with a vertical dimension of 100 m, a hydraulic head gradient of 1 % yields 1-m total head change. The measured heads will vary within ± 1 cm of the true hydraulic head values. Because modern tapes and pressure transducers can yield observed heads with a precision of <1 cm (Post and von Asmuth 2013), the head measurement errors imposed are considered reasonable. To facilitate the interpretation of the inverse solution, Darcy fluxes sampled from the FDM are not corrupted by errors. In Jiao and Zhang 2014b, for example, inverse analyses imposing errors on both measured heads and measured fluxes yielded stable and reasonable solutions, when compared to those where only hydraulic heads were imposed with errors.

Deterministic inversion

For two of the forward models (Table 1), three inverse analyses are carried out: cases 1, 2, and 3. Information about the observations used in the inverse model, the inversion grid, and the type of conductivity parameterization is shown in Table 2. Each inversion grid has a regular cell spacing. The observed data were sampled from the FDM at regular intervals.

In the first problem (case 1), the forward model of case (A) is inverted with piecewise continuous parameterization for K; one $K(z)$ function is inverted for each inversion grid cell. To the observed heads sampled from the FDM, increasing measurement errors (0, ± 0.1, and ± 1 %) are imposed. The
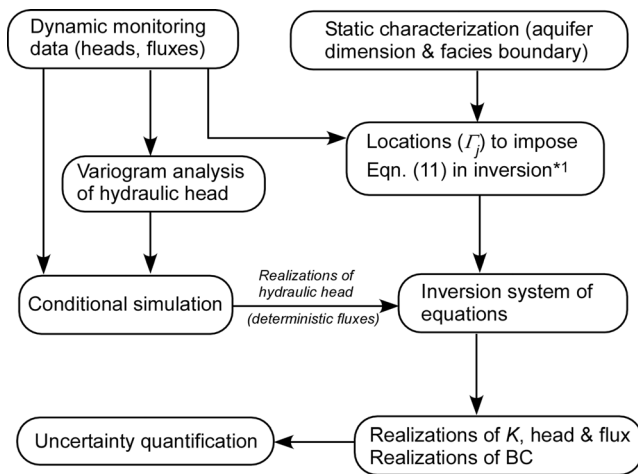
*1 Eqn. (11) is not used when K is piecewise constant.

Fig. 1 Stochastic inversion for uncertainty quantification of the estimated parameters and flow field. For conditional simulation of the observed hydraulic head, an exponential model is fitted to the experimental variogram of the hydraulic head

inverted hydraulic heads and estimated K profiles are shown in Fig. 2a,b, respectively. Under the increasingly larger head errors, the inverted heads are all close to the true heads of the FDM. The largest measurement errors only lead to slight fluctuations of the inverted heads from the true heads. Conductivity estimation, however, is more sensitive to the head errors: when measurements are error-free, the inverted conductivities are close to the true K profile (labeled as FDM); when measurement errors are increased, the inverted conductivities increasingly deviate from the true K profile. Despite the imposed errors, all inverse solutions are stable: estimation errors for either the inverted heads or the inverted K remain bounded.

In case 2, two facies zones exist in the FDM (case B), which are separated by a discontinuity at the facies boundary. Within each facies, K exhibits a continuous profile. In inversion, the same observation locations and the inversion grid of case 1 are used. Increasing errors (0, ±0.1, and ±1 %) are also imposed on the observed heads. Conductivity in inversion is formulated as piecewise continuous. Location of the facies boundary is assumed to be known in the inverse model, i.e., the location where Eq. (11) is *not* imposed is known. In practice, such locations can be inferred from where abrupt change in the gradients of the observed hydraulic heads occurs. (Alternatively, such information can be inferred from independent data such as downhole lithology logs or wireline geophysical data). The location of the facies boundary helps to design the inversion grid where this boundary coincides with a cell interface, which ensures that no single $K(z)$ function spans the boundary. Also, for this problem, Eq. (11) is not enforced at this interface, while it is enforced elsewhere in the inversion domain to represent within-facies K variations, i.e., $X=Y-1$.

Results of the inverted hydraulic head and conductivity profiles are shown in Fig. 3. For all levels of the imposed measurement errors, the inverted heads are very close to the FDM true profile. When measurements are error-free,

the inverted conductivities are close to those of the FDM. When measurement errors are increased, the inverted conductivities exhibit increasing deviations from the true K profile. This deviation is the most pronounced within the higher conductivity facies. This is because the same magnitude of measurement errors are imposed onto the observed heads throughout the inversion domain, while the total head variation is smaller in the high-K facies than in the low-K facies. In the high-K facies, the local head errors are comparably of higher magnitude, which leads to greater local K estimation errors. These errors, however, remain bounded as the estimated K fluctuates around the true K profile. The inverse solutions are thus considered stable under increasing measurement errors.

In case 3, the FDM of case (A) is inverted again using error-free measurements, while K is alternatively parameterized as piecewise continuous and piecewise constant. For the first parameterization, 30 heads and 10 fluxes are sampled as measurements, for which Eqs. (4)–(11) are assembled and solved; for the second parameterization, 100 heads and 100 fluxes are sampled (to ensure that the inverse system of equations is over-determined) and Eqs. (4)–(10) are assembled and solved. The inversion results are shown in Fig. 4. For both parameterizations, the inverted hydraulic heads are extremely close to the true heads of the FDM. However, the inverted K profiles differ to a much greater extent: despite the greater number of measurements used, the inverted conductivities with piecewise constant parameterization are less accurate than those with piecewise continuous parameterization. Conductivity estimation error of the former also appears to increase with increasing magnitude of the K, while this effect is absent in the K profile inverted with the latter formulation. Piecewise continuous parameterization thus yields more accurate and stable outcomes while requiring fewer measurements.

Stochastic inversion
The inverse method is combined with geostatistical simulation to estimate a set of stochastic ensemble of the inverted hydraulic heads and conductivities. Four inversion cases are tested (cases 4–7), and information about each case is shown in Table 3. Compared to the preceding deterministic inversion, fewer observations are needed in stochastic inversion of the same FDM, because more hydraulic heads, created by conditional simulation, are used by the inverse model. The expanded "measurement" data thus contribute to the well-posedness of the inverse equation systems, although deviation of the geostatistically simulated heads from the true head profile will contribute to estimation errors in inversion. Such errors, however, can be used to define the uncertainty in estimation, as explained in the following paragraphs. Moreover, both K parameterization schemes are tested; compared to piecewise continuous parameterization, when K is assumed as piecewise constant, more measurements are needed for the inversion to yield stable solutions.

In case 4, the FDM of case (A) is inverted. From the FDM, 10 observed heads and 9 observed fluxes are sampled

Table 1 One-dimensional forward models developed in this study to test the inverse theory. To ensure accuracy in the forward solutions, dense grids are used to discretize the FDM

FDM	Conductivity distribution (cm/day)	Computational domain (cm)	Boundary condition (cm)	Number of grid cells
Case (A)	$9\sin\left(\frac{\pi z}{1,000}\right) + 1$	[0, 1,000]	$h(0) = 10$, $h(1,000) = 20$	2,000
Case (B)	K1(z): $9\sin\left(\frac{\pi z}{500}\right) + 10$	K1(z): [0, 500]	$h(0) = 10$, $h(1,000) = 20$	5,000
	K2(z): $9\sin\left(\frac{\pi z}{500} - 1\right) + 30$	K2(z): [500, 1,000]		
Case (C)	$99\sin\left(\frac{\pi z}{1,000}\right) + 1$	[0, 1,000]	$h(0) = 10$, $h(1,000) = 20$	5,000

at regular intervals. Given the observed heads, an exponential model is fitted to the experimental variogram, based on which 100 hydraulic head conditional realizations are generated. From each realization, 27 simulated hydraulic heads, sampled at regular intervals, are used by the inverse model in addition to the flux measurements (Table 3). Using the piecewise continuous formulation, these measurements are inverted to create one realization of the hydraulic head and conductivity profiles. Given 100 realizations of the simulated heads (i.e., the locations of the simulated heads used by the inverse model remain identical), 100 sets of inverted heads and conductivities are obtained.

A similar stochastic inversion procedure is then carried out for cases 5–7. In case 5, the problem of case 4 is repeated, although the number of observed heads is doubled to 20. As a well-known result in geostatistics, the extra measured heads will lead to reduced uncertainty in the conditionally simulated heads (i.e., a smaller standard deviation in the hydraulic head ensemble at each simulated location), thus reducing deviation of the simulated heads from the true heads. In inversion, 27 simulated heads are again used (as in case 4).

Figures 5 and 6 present the 100 realizations of the inverted heads and conductivities for cases 4 and 5, respectively. The FDM heads and conductivities are plotted for comparisons. Compared to case 4, because more observed heads are used in conditional simulation (even though the total number of heads used by the inverse model is the same), the inverted heads and conductivities of case 5 are more accurate, i.e., on average, smaller standard deviations are observed from the true heads and conductivities at individual inversion grid cells. This is confirmed by the computed calibration uncertainties at the location of the observed heads: $\sigma_{nh} = 1.35 \times 10^{-2}$, $\sigma_{nK} = 6.17$ (case 4) and $\sigma_{nh} = 3.73 \times 10^{-3}$, $\sigma_{nK} = 1.88$ (case 5). Moreover, the inverted conductivity profiles of both case 4 (Fig. 5b) and

case 5 (Fig. 6b) show regular and near linear fluctuations along the true K profile. This phenomenon is a result of the periodic head fluctuations in the conditionally simulated head profile (not shown): such fluctuation occurs along the true head profile at regular intervals, yielding fluctuating hydraulic gradient, which results in fluctuation in the estimated K. Had a different stochastic technique been used (e.g., one that dampens the head fluctuation in conditional simulation), the characteristics of the inverted K field will likely change.

In case 6, the FDM case (C) is inverted with piecewise continuous parameterization (Fig. 7). Compared to case 5, the number of measurements used and the inversion grid are the same. Again, 100 conditionally simulated head profiles are generated. From each realization, 27 simulated heads are sampled and subsequently used by the inverse model. In case 6, heterogeneity level of the FDM is greater than that of case 5: $K_{max}/K_{min} = 100$ (case 6) and 10 (case 5). Comparing Figs. 6 and 7, uncertainty in the inverse solution (i.e., spread of the inverted K and heads from the true K and heads) is found insensitive to the change in the conductivity contrast. This is confirmed by the calibration uncertainties (at the same observed head location): $\sigma_{nh} = 3.73 \times 10^{-3}$, $\sigma_{nK} = 1.88$ (case 5) and $\sigma_{nh} = 3.35 \times 10^{-3}$, $\sigma_{nK} = 2.1$ (case 6). Given the piecewise continuous parameterization, the inverse method is stable for the different conductivity models tested, i.e., the ensemble K and head fields remain bounded.

In case 7, the FDM of case (A) is inverted with piecewise constant parameterization (Fig. 8). The number of measurements used and the inversion grid discretization are shown in Table 3. Compared to case 5, the same number of observed heads is sampled. Because of the greater number of unknowns that are sought in inversion, 45 simulated heads are used by the inverse model, and many more fluxes are also sampled from the FDM. Comparing Figs. 6a and 8a, the inverted hydraulic heads

Table 2 Deterministic inversion problems tested in this study

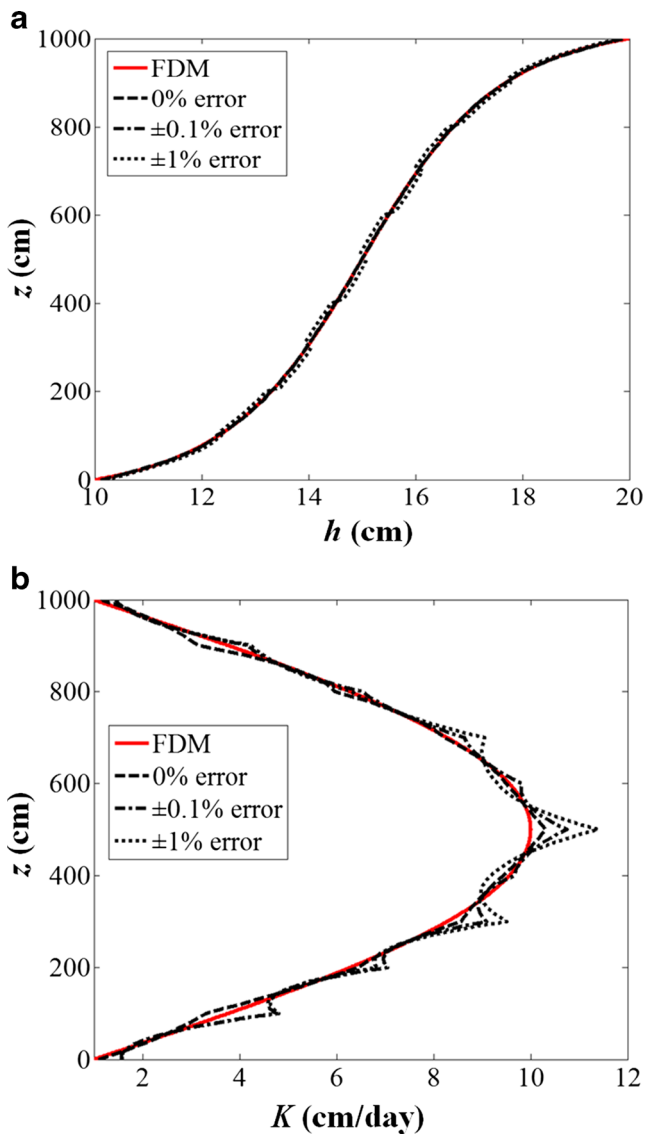| Inversion	FDM (true model)	Parameterization	Observed data sampled from FDM	Number of inversion grid cells
Case 1	Case (A)	Piecewise continuous	30 heads, 10 fluxes	10
Case 2	Case (B)	Piecewise continuous	30 heads, 10 fluxes	10
Case 3	Case (A)	Piecewise constant	100 heads, 100 fluxes	100
		Piecewise continuous	30 heads, 10 fluxes	10

Fig. 2 Case 1: **a** FDM hydraulic heads versus inverted hydraulic heads under increasing measurement errors; **b** FDM conductivities versus inverted conductivities under increasing measurement errors
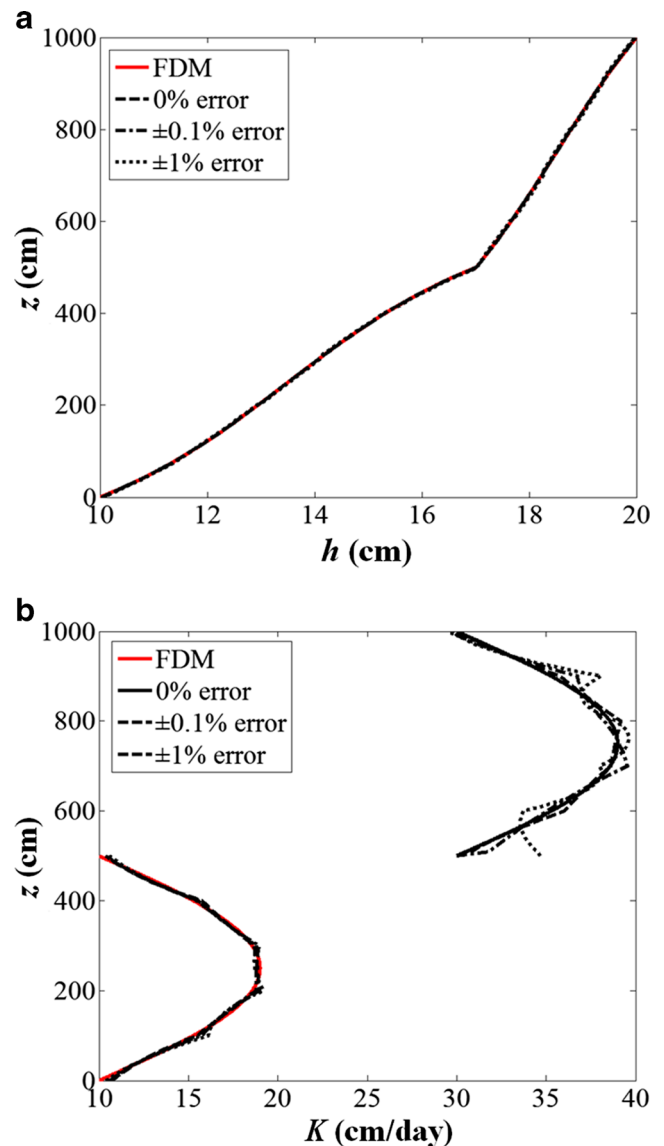

Fig. 3 Case 2: **a** FDM hydraulic heads versus inverted hydraulic heads under increasing measurement errors; **b** FDM conductivities versus inverted conductivities under increasing measurement errors

are close to the FDM true heads. Calibration uncertainties of the inverted heads and conductivities are: $\sigma_{nh} = 3.73 \times 10^{-3}$, $\sigma_{nK} = 1.88$ (case 5) and $\sigma_{nh} = 2.53 \times 10^{-3}$, $\sigma_{nK} = 13.99$ (case 7). Comparing Figs. 6b and 8b, however, the inverted conductivities with piecewise constant parameterization exhibit much larger fluctuations (i.e., average standard deviation of the ensemble) compared to those inverted with piecewise continuous parameterization. Again, in stochastic inversion, piecewise continuous parameterization yields better outcomes while requiring fewer measurements.

Discussion

To capture heterogeneity where K exhibits irregular or abrupt changes corresponding to within- or between-facies

variations, this research extends earlier studies where a direct method was developed for steady-state and transient flow inversion under unknown boundary and/or initial conditions. A set of continuity, data, and equation constraints is imposed to ensure that the inverse solution is physically based. However, instead of zonation, K is parameterized as piecewise continuous or piecewise constant. In the first parameterization, to ensure a well-posed solution (i.e., stable inversion generally requires an exact or over-determined system of equations) and to reduce inversion artifacts (e.g., K fluctuation in response to measurement errors in the observed heads and/or fluxes), an additional continuity constraint is added to enforce smoothness of K at the interfaces between adjacent inversion cells (but not at facies boundaries, where abrupt change in K is expected). To assess uncertainty in inversion and to further reduce data requirement, the inverse method is combined with geostatistical conditional simulation
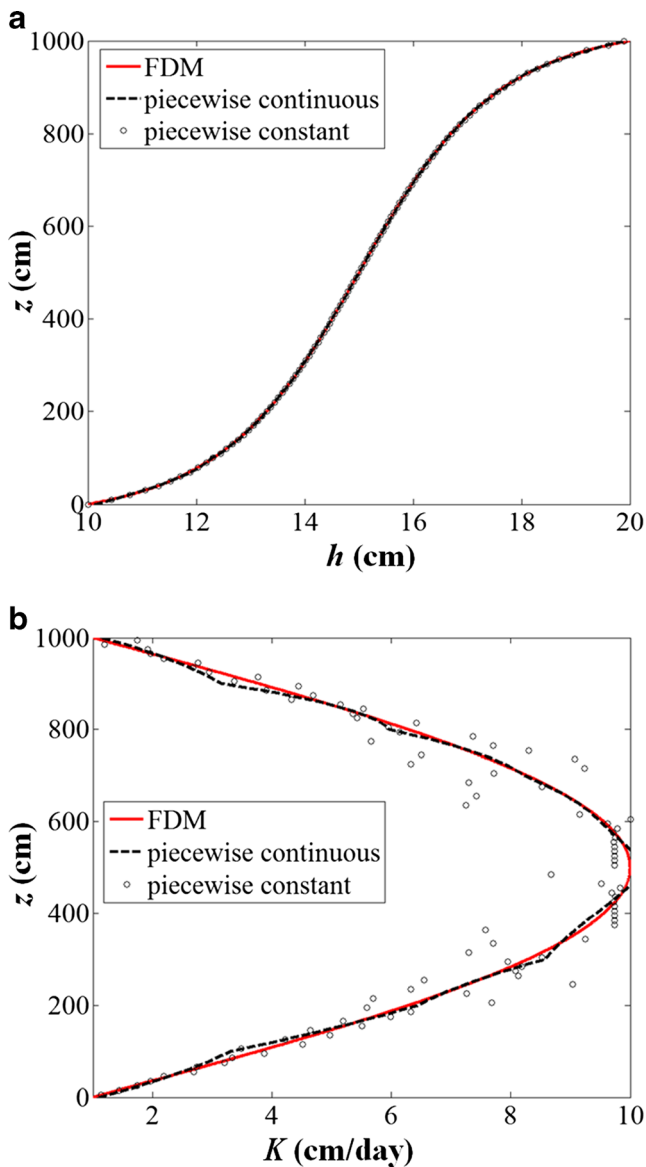
Fig. 5 Case 4: **a** FDM hydraulic heads (*black dash curve*) versus 100 inverted hydraulic heads profiles (*grey curves*); **b** FDM conductivities (*black dash curve*) versus 100 inverted conductivities profiles (*grey curves*)

Fig. 4 Case 3: **a** Inverted hydraulic heads under piecewise continuous vs constant parameterization with error-free measurement; **b** Inverted conductivities based on piecewise continuous vs constant parameterization with error-free measurement

to yield realizations of the inverted K and hydraulic head fields. From these realizations, the unknown BC and their uncertainties can also be quantified by sampling the appropriate state variables (not shown).
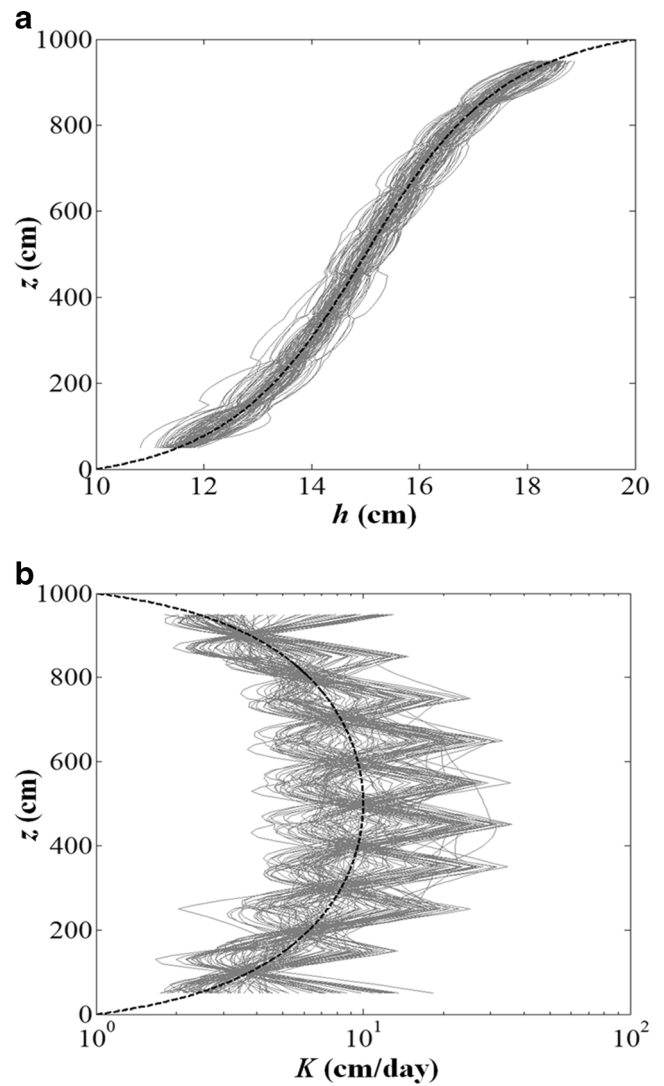
By designing a set of synthetic examples, a forward FDM is used to provide measurements for inversion as well as acting as the ground truth against which each inverse solution is evaluated. Results suggest that the LAS inverse method can lead to stable inversion under increasing measurement errors. The combination of

Table 3 Stochastic inversion problems tested in this study

Inversion	FDM	Observations (error-free) from the FDM	Parameterization	Observations that are used by the inverse model	Number of inversion grid cells
Case 4	Case (A)	10 heads[a], 9 fluxes	Piecewise continuous	27 heads[b], 9 fluxes[c]	9
Case 5	Case (A)	20 heads, 9 fluxes	Piecewise continuous	27 heads, 9 fluxes	9
Case 6	Case (C)	20 heads, 9 fluxes	Piecewise continuous	27 heads, 9 fluxes	9
Case 7	Case (A)	20 heads, 45 fluxes	Piecewise constant	45 heads, 45 fluxes	45

[a] Error-free observations are sampled from the FDM at regular intervals, which are used to condition the geostatistical simulations of the head profile

[b] Hydraulic heads sampled from a conditionally simulated head profile at regular intervals

[c] Flux measurements that are used by the inverse model are deterministic and are the same as those sampled from the FDM
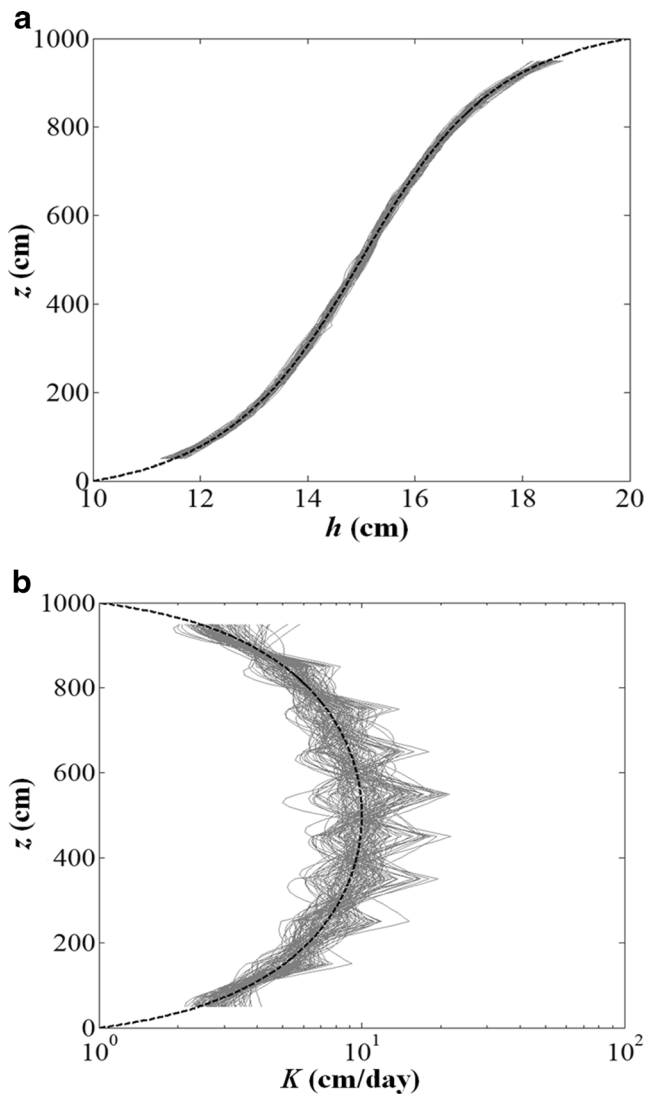
Fig. 6 Case 5: **a** FDM hydraulic heads (*black dash curve*) versus 100 inverted hydraulic heads profiles (*grey curves*); **b** FDM conductivities (*black dash curve*) versus 100 inverted conductivities profiles (*grey curves*)

Fig. 7 Case 6: **a** FDM hydraulic heads (*black dash curve*) versus 100 inverted hydraulic heads profiles (*grey curves*); **b** FDM conductivities (*black dash curve*) versus 100 inverted conductivities profiles (*grey curves*)
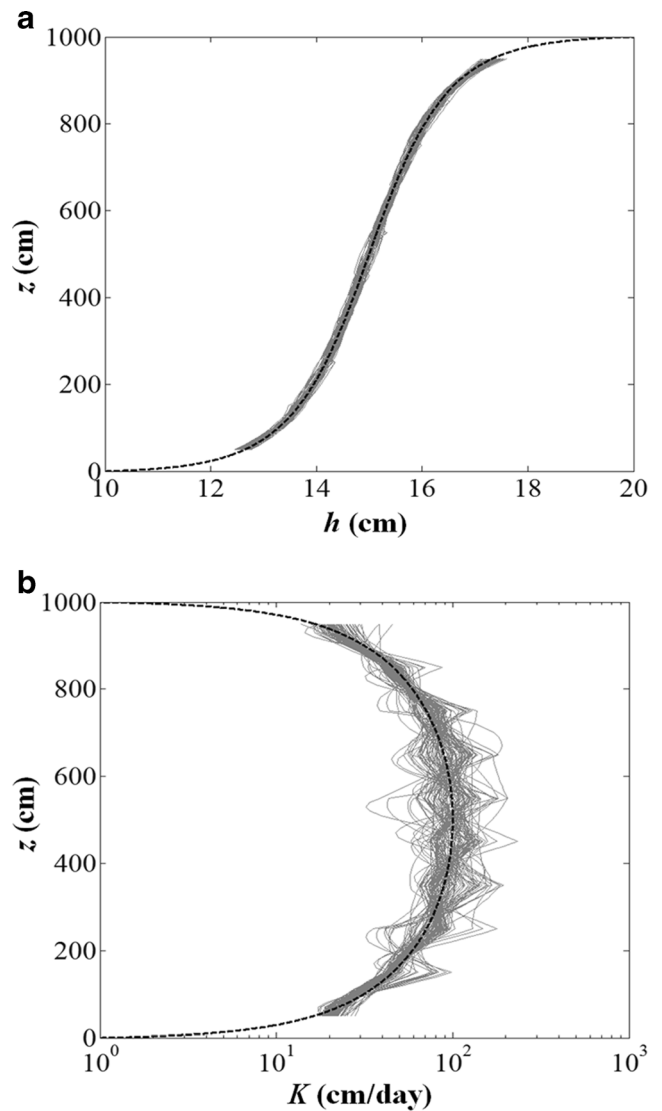
piecewise continuous K formulation with the (local) K continuity constraint can realistically capture aquifer of aquifer heterogeneity including abrupt facies changes, without resorting to zonation. However, for inverting a problem with two facies, location of the facies boundary was assumed *known* in the inverse model, where the local K continuity constraint was *not* imposed. While facies boundaries may be ascertained from indirect data (e.g., porosity or lithology logs), it is of interest to invert problems where the location of facies may be difficult to determine from existing data. Also, for the two-facies problem, K was smoothly varying within each facies. It is of interest to invert problems where sub-facies K varies irregularly. Using the piecewise continuous formulation, a segment of hydraulic conductivity profile from an oil field (Rogers et al. 1995) is inverted by assuming synthetic fluid flow boundary conditions for the forward model. The conductivity profile (Fig. 9b; solid curve) exhibit

three district facies, while within-facies K varies irregularly. To solve this problem, the inversion grid is first designed by examining the (true) hydraulic head profile simulated by the forward model, from which six points can be identified where dh/dz change is significant (Fig. 9a). Based on these locations, an irregular inversion grid with seven cells is created, with cell sizes corresponding to the observed z intervals with relatively constant dh/dz. From the forward model, error-free measurements are sampled randomly while satisfying this criterion: at least three heads and three fluxes are sampled for each inversion cell (a total of 21 heads and 21 fluxes are sampled). Because the true K profile exhibits strong variability at small scales, the K continuity constraint (i.e., Eq. 11) is *not* imposed. The inverted head profile is very accurate (Fig. 9a), while the inverted conductivities are smooth varying, following the mean fluctuation of the
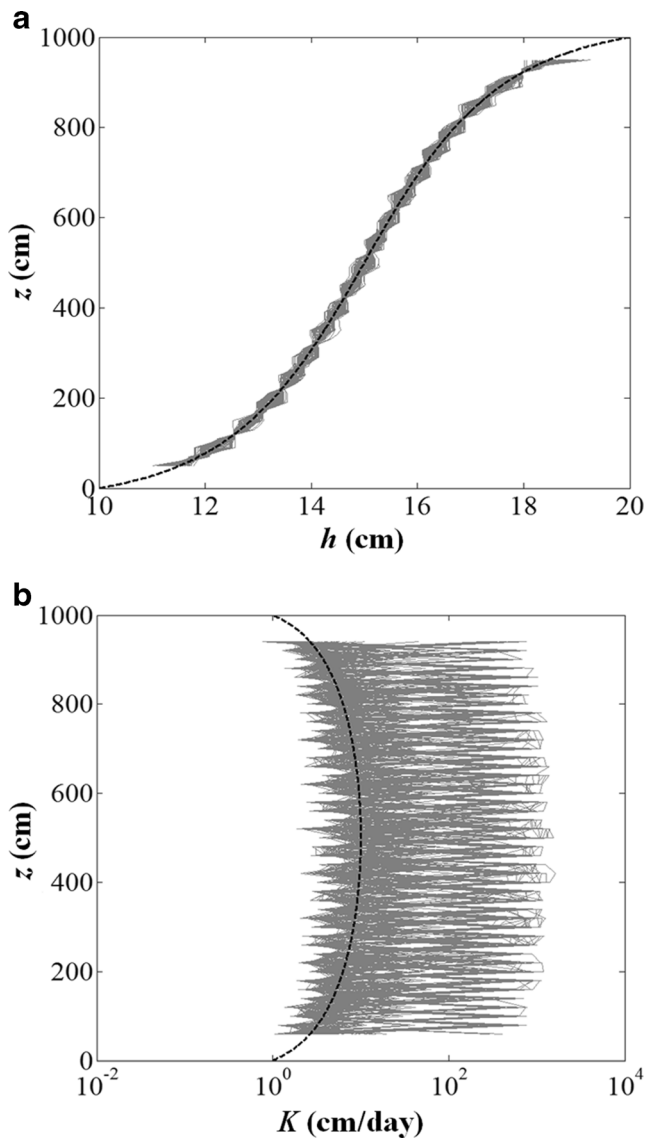
Fig. 8 Case 7: **a** FDM hydraulic heads (*black dash curve*) versus 100 inverted hydraulic heads profiles (*grey curves*); **b** FDM conductivities (*black dash curve*) versus 100 inverted conductivities profiles (*grey curves*)

dh/dz changes. In this case, the grid is the least amenable to accurate inversion. Measurements of the first problem (21 heads and 21 fluxes) and the second problem (21 heads and 24 fluxes) are then provided. Both lead to less accurate inversion, as expected. Figure 9e,f provides the results when measurements of the first problem were used. The worsened performance is expected for K estimation, although head estimation is less influenced by the new grid. Overall, reasonable inversion outcomes can be obtained for the realistic conductivity data with the method of this study.

When the new inverse method is combined with conditional simulation, it leads to reduced data requirement compared to deterministic inversion although this is at the cost of creating uncertainty in estimation. Clearly, whether deterministic or stochastic inversion is preferable depends on the availability of the measurements. With fewer measurements, the stochastic approach can yield inversion outcomes with a larger degree of uncertainty which can be quantified from the ensembles of the inverted K and head fields. With more measurements, modelers may choose to adopt the deterministic approach, although such an approach (with piecewise continuous parameterization) still requires a *sufficient* number of measurements. How sufficient the measurements are can be determined by examining the rank of the inverse equations. (Optimization solvers for undetermined systems do exist, and future work will test alternative solvers to evaluate whether the data requirement can be further reduced.) Finally, as the preprocessor for inversion, only hydraulic heads are simulated by conditional simulation. Future work will explore co-simulation techniques so that other data (e.g., local K measurements, lithology data, geophysical measurements) can be incorporated into the stochastic conditioning process. The ultimate limitation to the wider application of the proposed inverse method, the authors believe, is data limitation. When data, whether static or dynamic, are too limited, geostatistical techniques will not likely lead to improved outcomes compared to deterministic inversion.

Conclusion

The LAS inverse method using piecewise functional K is introduced for inverting steady-state flow in heterogeneous aquifers. By combining inversion with geostatistical conditional simulation, estimation uncertainty can be quantified. In the stochastic procedure, observed hydraulic head distribution is modeled and used to condition the inversion, which leads to ensemble fields of the inverted hydraulic heads and Ks. Based on numerical experiments, the inversion outcomes are verified and their accuracy and stability evaluated against the forward models. Key results of this study are summarized as follows:

- The inverse method with continuous parameterization is accomplished by imposing 4 constraints: (1) spatial
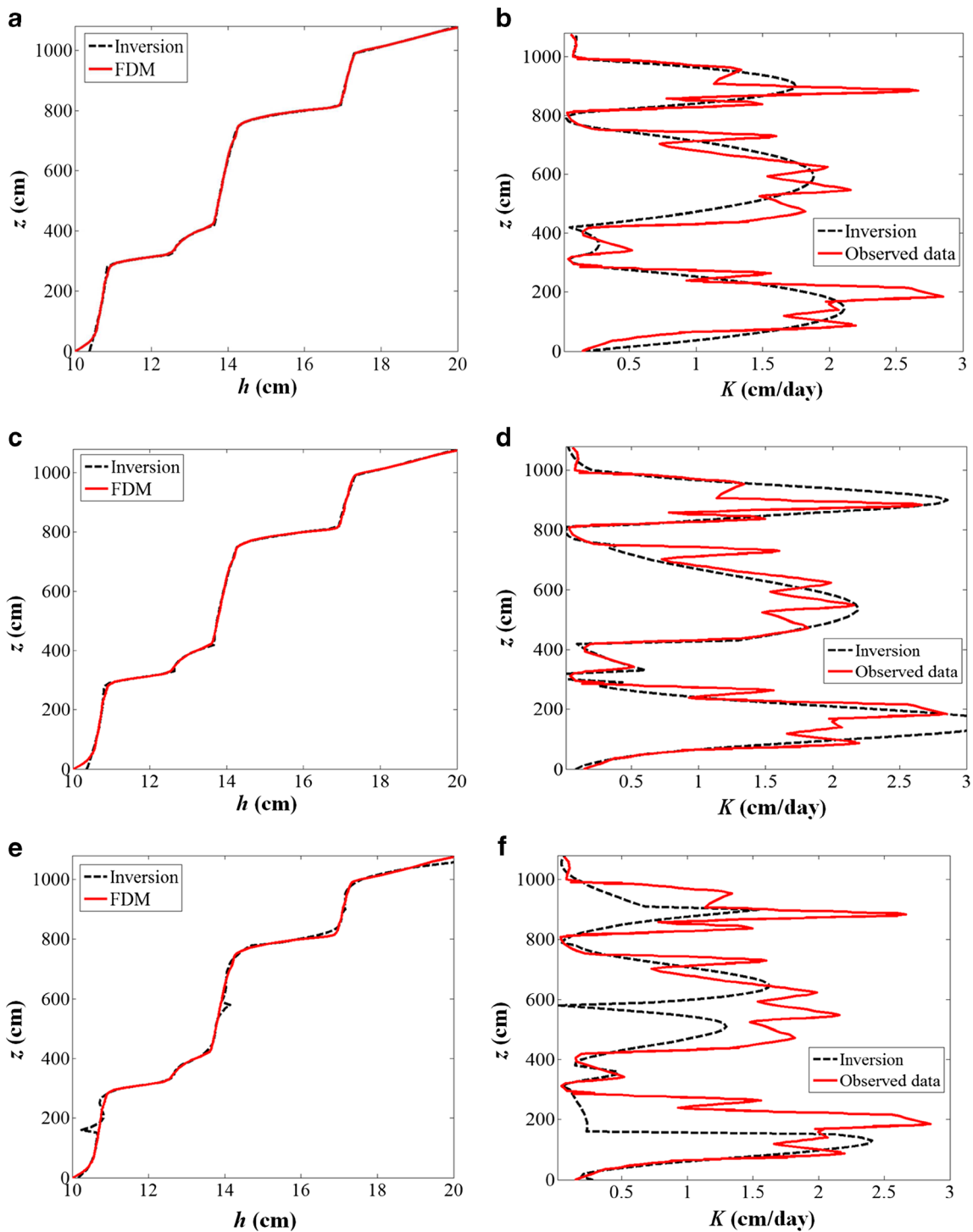
true profile (Fig. 9b). This is likely a result of the proposed LAS for conductivity (Eq. 15), which is smooth varying. The inverted K fails to capture the two peaks at $z=183.86$ and $z=880.37$ cm, where it underestimates the true values by 20–45 %. To see if this issue can be addressed with additional sampling, the aforementioned analysis is repeated using the same inversion grid and measurements, except for three additional fluxes that are sampled at $z=183.86$, 547.45, and 880.37 cm, i.e., locations of peak K values in the facies. Results (Fig. 9c,d) suggest that K estimation (Fig. 9d) improves at these locations, although due to the nature of the LAS of K, small fluctuations at the sub-facies scale cannot be captured well. Moreover, a problem is investigated where the locations with significant *dh/dz* changes are unknown. A non-uniform inversion grid with seven cells is developed, where *all* cell interfaces do not correspond to

Fig. 9 **a**, **c**, **e** FDM hydraulic heads (*solid red curve*) versus inverted hydraulic heads (*dashed curves*): **a** known locations of facies transition; **c** known locations of both facies transition and the maximum K within each facies; **e** unknown locations of both facies transition and maximum K within each facies; **b**, **d**, **f** true K profile (*solid red curve*) versus inverted K profile (*dashed curve*); **b** known locations of facies transition; **d** known locations of both facies transition and the maximum K within each facies; **f** unknown locations of both facies transition and maximum K within each facies

continuity of hydraulic head and Darcy fluxes; (2) conditioning of the LAS to observed data; (3) equation constraints at selected spatial locations to enforce flow physics; and (4) local K continuity constraint to enforce smoothness on small-scale K variation.

- Given the piecewise continuous parameterization, constraint (4) is needed to reduce artifacts in inversion and to ensure that the inverse system of equation is well-posed. Abrupt conductivity changes due to facies changes can also be captured, although constraint (4)

should be removed at the locations corresponding to facies changes to ensure accuracy.

- As a subset of the functional parameterization, the piecewise constant formulation (which is similar to highly parameterized inversion, and the local K continuity constraint is removed) leads to less accurate K estimation while requiring higher measurement supports. In comparison, piecewise continuous parameterization leads to more stable and accurate inversion while requiring fewer measurements.
- When increasing measurement errors are imposed on the observed heads, the estimated conductivities become less accurate, but the inverse solution is still stable, i.e., estimation errors remain bounded.
- In stochastic inversion with piecewise continuous parameterization, inversion improves with increasing number of the observed heads. Given the same measurement support, inversion outcomes are insensitive to conductivity contrast, i.e., K_{max}/K_{min} is tested up to 100.

In this study, measurement data that are used by the inverse model include hydraulic heads and Darcy fluxes. While heads can be easily sampled with pressure transducers, in-situ flux sampling requires specialized techniques (Labaky et al. 2009). Future work will extend the method of this study to higher spatial dimensions and to transient flows. Pattern recognition will be investigated, with which location and shape of the facies can be inferred from the solution. Joint inversion will also be explored, e.g., co-simulation of hydrological data with indirect data such as lithology logs or geophysical measurements.

References

Anderson MP (1997) Characterization of geological heterogeneity. In: Subsurface flow and transport: a stochastic approach. Cambridge University Press, Cambridge, UK, pp 23–43

Amudo C, Graf T, Harris NR, Dandekar R, Amor FB, May R S (2008) Experimental design and response surface models as a basis for stochastic history matching: a Niger Delta experience. SPE paper no. 12665, SPE, Richardson, TX

Capilla JE, Rodrigo J, Gomez-Hernandez JJ (1999) Simulation of non-Gaussian transmissivity fields honoring piezometric data and integrating soft and secondary information. Math Geol 31(7):907–927

Carrera JY, Neuman SP (1986a) Estimation of aquifer parameters under steady-state and transient conditions: I. background and statistical framework. Water Resour Res 22(2):199–210

Carrera JY, Neuman SP (1986b) Estimation of aquifer parameters under steady-state and transient conditions: II. uniqueness, stability, and solution algorithms. Water Resour Res 22(2):211–227

Carrera JY, Neuman SP (1986c) Estimation of aquifer parameters under steady-state and transient conditions: III. applications. Water Resour Res 22(2):228–242

Carrera J, Alcolea A, Medina A, Hidalgo J, Slooten LJ (2005) Inverse problem in hydrogeology. Hydrogeol J 13:206–222

Deutsch CV, Journel AG (1994) Integrating well test-derived effective absolute permeabilities in geostatistical reservoir modeling. In: Yarus JM, Chambers RL (eds) Stochastic modeling and geostatistics, vol 3. AAPG, Tulsa, OK, pp 131–142

Doherty J (2005) PEST: Software for model-independent parameter estimation, Watermark Numerical Computing, Brisbane, Australia. http://www.pesthomepage.org/Home.php. Accessed October 2013.

Eide A L, Holden L, Reiso E, Aanonsen SI (1994) Automatic history-matching by use of response surfaces and experimental design. Proceedings, 4th European Conference on the Mathematics of Oil Recovery, Roros, Norway, June 1994

Eppstein MJ, Dougherty DE (1996) Simultaneous estimation of transmissivity values and zonation. Water Resour Res 32(11):3321–3336

Ferraresi M, Todini E, Vignoli R (1996) A solution to the inverse problem in groundwater hydrology based on Kalman filtering. J Hydrol 175:567–581

Fogg GE (1990) Architecture and interconnectedness of geologic media: role of the low-permeability facies in flow and transport. Heise, Hannover, Germany, pp 19–40

Gallo YL, Ravalec-Dupin ML (2000) History matching geostatistical reservoir models with gradual deformation method. Proceedings, 1st International Energy Agency Workshop and Symposium, Edinburgh, UK, September 20–22, 2000

Gelhar LW (1992) Stochastic subsurface hydrology, Prentice Hall, Upper Saddle River, NJ, 480 pp

Ginn TR, Cushman JH (1990) Inverse methods for subsurface flow: a critical review of stochastic techniques. Stoch Hydrol Hydraul 4(1):1–26

Hill MC (1992) A computer program (MODFLOWP) for estimating parameters of a transient, three dimensional, groundwater flow model using nonlinear regression. US Geol Surv Open File Rep 91-484

Hill MC, Tiedeman CR (2007) Effective groundwater model calibration: with analysis of data, sensitivities, predictions, and uncertainty. Wiley, New York, 480 pp

Irsa J, Zhang Y (2012) A new direct method of parameter estimation for steady state flow in heterogeneous aquifers with unknown boundary conditions. Water Resour Res 48, W09526. doi:10.1029/2011WR011,756

Janssen GMCM, Valstar JR, Sjoerd EA, van der Zee TM (2006) Inverse modeling of multimodal conductivity distributions. Water Resour Res 42, W03410. doi:10.1029/2005WR004356

Jiao JY, Zhang Y (2014a) Two-dimensional inversion of confined and unconfined aquifers under unknown boundary condition. Adv Water Resour 65:43–57

Jiao JY, Zhang Y (2014b) Tensor hydraulic conductivity estimation for heterogeneous aquifers under unknown boundary conditions. Groundwater. doi:10.1111/gwat.12202

Jiao JY, Zhang Y (2014c) A method based on Local Approximate Solutions (LAS) for inverting transient flow in heterogeneous aquifers. J Hydrol. doi:10.1016/j.hydrol.2014.04.004

Kitanidis PK (1995) Quasi-linear geostatistical theory for inversing. Water Resour Res 31(10):2411–2419

Kromah MJ, Liou J, MacDonald DG (2005) Step change in reservoir simulation breathes life into mature oil field. SPE paper no. 94940, SPE, Richardson, TX

Labaky W, Devlin JF, Gillham RW (2009) Field comparison of the point velocity probe with other groundwater velocity measurement method. Water Resour Res 45, W00D30. doi:10.1029/2008WR007066

LaVenue AM, Pickens JF (1992) Application of a coupled adjoint sensitivity and kriging approach to calibrate a groundwater model. Water Resour Res 28(6):1543–1570

McLaughlin D, Townley LR (1996) A reassessment of the groundwater inverse problem. Water Resour Res 32(5):1131–1161

McKenna SA, Poeter EP (1995) Field example of data fusion in site characterization. Water Resour Res 31(12):3229–3240

610

Medina A, Carrera J (2003) Geostatistical inversion of coupled problems: dealing with computational burden and different type of data. J Hydrol 281(4):251–264

Poeter EP, Hill MC, Banta ER, Mehl S, Christensen S (2005) UCODE_2005 and six other computer codes for universal sensitivity analysis, calibration, and uncertainty evaluation. USGS Techniques and Methods, 6-A11, USGS, Reston, VA, 283 pp

Porter DW, Gibbs BP, Jones WF, Huyakorn PS, Hamm LL, Flach GP (2000) Data fusion modeling for groundwater systems. J Contam Hydrol 42:303–335

Post VEA, von Asmuth JR (2013) Review: hydraulic head measurements: new technologies, classic pitfalls. Hydrogeol J 21:737–750

Ramanathan R, Guin A, Ritzi RW et al (2010) Simulating the heterogeneity in braided channel belt deposits: 1. a geometric-based methodology and code. Water Resour Res 46(4), W04515. doi:10.1029/2009WR008111

Rogers SJ, Chen HC, Kopaska-Merkel DC, Fang JH (1995) Predicting permeability from porosity using artificial neural networks. AAPG Bull 79(12):1786–1796

Roggero F, Hu LY (1998) Gradual deformation of continuous geostatistical models for history matching. SPE paper no. 49005, SPE, Richardson, TX

Romero CE, Carter JN, Zimmermann RW, Gringarten AC (2000) Improved reservoir characterization through evolutionary computation. SPE paper no. 62942, SPE, Richardson, TX

Sagar B, Yakowitz S, Duckstein L (1975) A direct method for the identification of the parameters of dynamic nonhomogeneous aquifers. Water Resour Res 11(4):563–570. doi:10.1029/WR011i004p00563

Sakaki T, Frippiat CC, Komatsu M, Illangasekare TH (2009) On the value of lithofacies data for improving groundwater flow model accuracy in a three-dimensional laboratory-scale synthetic aquifer. Water Resour Res 45, W11404. doi:10.1029/2008WR007229

Scheibe DT, Freyberg DL (1995) Use of sedimentological information for geometric simulation of natural porous media structure. Water Resour Res 31:3259–3270

Schulze-Riegert R, Axmann J, Haase O, Rian D, You Y (2002) Evolutionary algorithms applied to history matching of complex reservoirs. SPE Reserv Eval Eng 5(2):163–173

Tartakovsky DM (2013) Assessment and management of risk in subsurface hydrology: a review and perspective. Adv Water Resour 51:247–260

Vrugt JA, Stauffer PH, Wohling T, Robinson BA, Vesselinov VV (2008) Inverse modeling of subsurface flow and transport properties: a review with new developments. Vadose Zone J 7:843–864

Wen XH, Deutsch CV, Cullick AS, Reza ZA (2000) Integration of production data in generating reservoir models. Stanf Cent For Comput Geostat (CCG) Monogr Ser 1:205

Yeh WWG (1986) Review of parameter identification procedures in groundwater hydrology: the inverse problem. Water Resour Res 22(2):95–108

Yeh TCJ, Jin M, Hanna S (1996) An iterative stochastic inverse method: conditional effective transmissivity and hydraulic head fields. Water Resour Res 32(1):85–92

Zanini A, Kitanidis PK (2009) Geostatistical inversing for large-contrast transmissivity fields. Stoch Env Res Risk A 23:565–577

Zhang Y, Person M, Paola C, Gable CW, Wen X-H, Davis JM (2005) Geostatistical analysis of an experimental stratigraphy. Water Resour Res 41, W11416. doi:10.1029/2004WR003756

Zhang Y (2014) Nonlinear inversion of an unconfined aquifer: simultaneous estimation of heterogeneous hydraulic conductivities, recharge rates, and boundary conditions. Transp Porous Media 102:275–299. doi:10.1007/s11242-014-0275-x

Zhang Y, Irsa J, Jiao JY (2014) Three-dimensional aquifer inversion under unknown boundary conditions. J Hydrol 509:416–429. doi:10.1016/j.jhydrol.2013.11.024

Zhou H, Gomez-Hernandez JJ, Li L (2014) Inverse methods in hydrogeology: evolution and recent trends. Adv Water Resour 63:22–37

Zhu J, Yeh TCJ (2006) Analysis of hydraulic tomography using temporal moments of drawdown recovery data. Water Resour Res 42, W02403. doi:10.1029/2005WR004309

Zimmerman DA et al (1998) A comparison of seven geostatistically based inverse approaches to estimate transmissivities for modeling advective transport by groundwater flow. Water Resour Res 34(6):1373–1413